Bedload dynamics at the confluence of large rivers

Basic Information

Title:	Bedload dynamics at the confluence of large rivers
Project Number:	2015WA404B
Start Date:	3/1/2015
End Date:	2/28/2016
Funding Source:	104B
Congressional District:	Washington, 5
Research Category:	Water Quality
Focus Category:	Geomorphological Processes, Sediments, Hydrology
Descriptors:	None
Principal Investigators:	John Petrie, Balasingam Muhunthan

Publications

1. Shehata, M., J. Petrie, 2016, Hydrodynamics in the confluence of the Snake and Clearwater Rivers, in River Flow 2016, International Conference on Fluvial Hydraulics, IAHR, St. Louis, MO.
2. Shehata, M., J. Petrie, 2016, Mixing zone hydrodynamics in a large confluence: a case study at the confluence of the Snake and Clearwater Rivers, BioEarth Annual Meeting, Washington State University (February 2016).
3. Shehata, M., J. Petrie, 2016, Mixing zone hydrodynamics in a large confluence: a case study at the confluence of the Snake and Clearwater Rivers, Pacific Northwest Water Research Symposium, Oregon State University (April 2016).
4. Shehata, M. and J. Petrie, Hydrodynamics at a large river confluence under low flow conditions. (In preparation)

1. PROBLEM AND RESEARCH OBJECTIVES

1.1 Introduction

Rivers in the Pacific Northwest provide numerous benefits to society including hydropower, transportation, irrigation, and recreation. These human uses are often in conflict with natural fluvial and biological processes. Nowhere is this conflict more evident than the confluence of the Snake and Clearwater Rivers at the border of Washington and Idaho. These rivers have been impacted by humans in a myriad of ways including hydropower dams built upstream and downstream of the confluence, a levee system protecting the cities of Clarkston, WA and Lewiston, ID, and commercial ports in both cities. The lower Granite Dam creates a reservoir which begins near the downstream end of the confluence. Monitoring of the riverbed elevation since dam construction shows significant sediment deposited in the vicinity of the confluence of the Snake and Clearwater Rivers. This sedimentation has adverse effects on the navigability of shipping channels and the capacity of the rivers to pass floods. The historical solution to sedimentation problems at this location has been dredging (USACE 2014). Questions regarding the environmental impacts of dredging, particularly with respect to national water quality standards and endangered species, led to a lawsuit by environmental groups in 2002. The response to the lawsuit was the development of the Lower Snake River Programmatic Sediment Management Plan (USACE 2014), an adaptive plan that embraces a range of approaches to address sediment-related problems. Among the potential remediation actions are dredging, reservoir drawdown to flush sediments, and hydraulic structures such as dikes and weirs. These potential activities require careful consideration as each alternative may have unforeseen impacts. For example, drawdown of the reservoir in 1992 led to a local marina filing for bankruptcy (W. Keefer, personal communication, November 17, 2014). Knowledge of flow and sediment dynamics in the vicinity of the confluence is needed to predict channel response and evaluate alternatives to improve water quality, protect habitat, as well as protect infrastructure. Thus, the results of this project will assist reservoir operators, port managers, fish biologists, and town mangers.

Confluences are important features of river networks providing diverse flow conditions that influence physical channel processes and biological processes (Benda et al. 2004). Despite the importance of confluences to the fluvial environment, research on confluence dynamics received little attention until the end of the last century (Rice et al. 2008). Beginning with the work of Mosley (1976) and Best (1986, 1987, 1988), research has expanded and embraced a range of approaches from laboratory experiments (Best 1988; Leite Ribeiro et al. 2012) to field studies (Biron et al. 1993, 2002; Rhoads & Kenworthy 1998; Rhoads & Sukhodolov 2001; Sukhodolov & Rhoads 2001) and numerical investigations (Bradbrook et al. 2000; Constantinescu et al. 2011, 2012). While these studies and others form the basis of our understanding of confluence dynamics, the vast majority of investigations consider confluences of small channels (channel width < 10 m). Only recently have confluences of large rivers (channel width > 100 m), such as the Snake and Clearwater Rivers, been the subject of detailed investigations (*e.g.*, Lane et al. 2008; Szupiany et al. 2009). These studies suggest important differences between small and large channels. To build a more complete understanding of confluences dynamics embracing the full range of scales requires significantly more observations from large channels (Parsons et al. 2008).

Confluence dynamics are influenced by the geometry of the joining channels as well as differences in the flow and sediment load. While the flows are of similar order of magnitude, recent

measurements have found that the Snake River carries more sediment than the Clearwater River with the Snake contributing as much as 90% of the sediment that deposits in the lower Granite Reservoir (Clark et al. 2013, see Figure 1). This difference in load has implications for sedimentation at the confluence as sediment transport is the link between flow structure and bed morphology (Best & Rhoads 2008). The total sediment load is often divided into the suspended load—finer material that moves in suspension—and bedload—coarser material that moves along the channel bottom. This study focuses on bedload due to evidence that much of the deposited material is coarse (Boll et al. 2010). At present, no direct observations of bedload dynamics have been reported in confluences of large rivers and only two studies have presented similar results for small channel confluences (Boyer et al. 2006; Rhoads 1996). Thus, this study seeks to make a fundamental contribution to our knowledge of confluence dynamics while addressing problems facing the confluence of the Snake and Clearwater Rivers.

Figure 1: The confluence of the Snake and Clearwater Rivers illustrating the difference in sediment load. The arrows indicate the direction of flow. (Photo courtesy of Wanda Keefer, Port of Clarkston)

1.2 Objectives

Our long-term goal is to develop a detailed understanding of flow and sediment processes and the resulting morphology at confluences of large rivers. The overarching goal of this project is to collect and analyze field data of flow and bedload transport in the confluence of the Snake and Clearwater Rivers. We propose to use state-of-the-art techniques to measure 3D velocity and bedload velocity using an acoustic Doppler current profiler (ADCP) at locations in the confluence region. The specific project objectives are:

1. *Quantify the 3D flow field at the confluence of two large rivers*. A boat-mounted ADCP will be used to measure velocity throughout the confluence of the Snake and Clearwater Rivers. Two survey methodologies will be used that allow for both spatially-rich and temporally-rich

velocity data. These measurements will be compared with previous measurements obtained at confluences of small rivers to clarify the role of scale on the flow field.

2. *Quantify bedload dynamics at the confluence of two large rivers*. Bedload transport characteristics will be measured at the field site using traditional, intrusive and cutting edge, nonintrusive methods. A Helley-Smith sampler will provide bulk measurements of the transport rate and the grain size distribution of the transported material. ADCP measurements and high resolution positioning will be used to determine the speed and direction of the transported bed material.

3. *Map spatial distribution of flow and sediment dynamics at the field site*. Results from the previous objectives will be compiled to produce vectors maps of flow and bedload transport. Viewing flow and sediment transport together at the field site allows the identification of regions where bedload is likely to be deposited and potential feedbacks between processes. These maps will be used to evaluate existing conceptual models for small channels confluences and contribute to the development of new models for large channel confluences.

1.3 Study area description

A field study was conducted in the large confluence of the Snake and the Clearwater Rivers adjacent to the towns of Clarkston, WA and Lewiston, ID (see
Figure 2) during the period of July 8-14, 2015. This confluence supports many purposes including commercial navigation, a downstream hydropower facility, as well as fish and wildlife conservation. As a consequence, the natural state of the confluence has been altered over time by a number of dredging operations performed to maintain the minimum navigable depth and adequate level of flood protection for the adjacent towns. The confluence is also influenced by backwater effects from the Lower Granite Reservoir (USACE 2014).

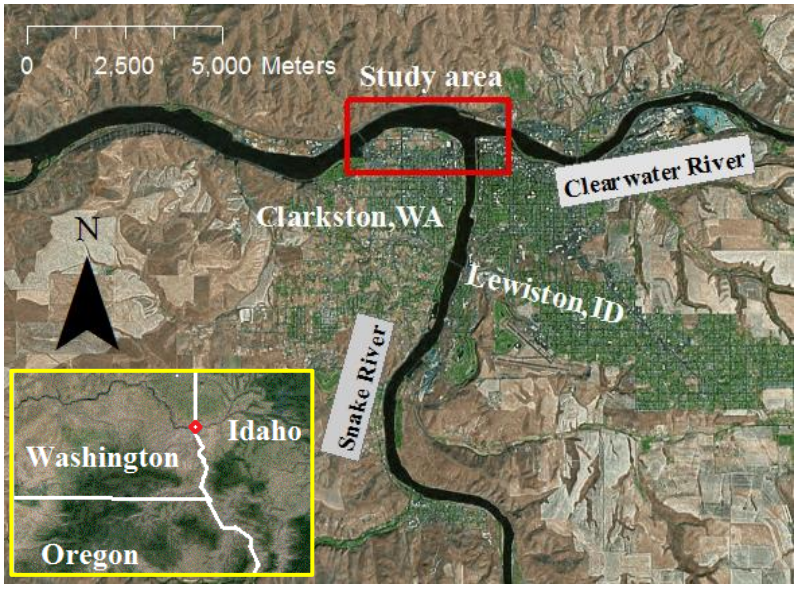

Figure 2: Location of the study site.

The average widths of the Snake and the Clearwater Rivers approaching the confluence are on the order of 300 m and the width increases to approximately 700 m in the confluence central zone. The two confluent rivers intersect at an angle of about 80 degrees. Two bridges exist at distances of ~450 m and ~600 m from the confluence upstream corner in the Snake and Clearwater Rivers, respectively. Another bridge crosses the post confluence region at a distance of ~3200 m from the upstream corner. The study area ends before the downstream bridge to avoid its artificial influence on the flow hydrodynamics.

In 2010, underwater video and surficial sediment cores were taken in the two confluent rivers and in the confluence zone by the USGS in cooperation with the USACE (Braun et al. 2012). The results indicate that the bed sediment in the confluence zone ranges from fine to medium sands with sizes mainly less than 0.5 mm in the regions near to the confluence upstream and downstream corners. The bed surface becomes coarser in the confluence central zone, which consists mainly of boulders, cobbles and gravels. Fine materials (silt and clay) were typically found to account for less than 20% and 40% of the surficial sediments in the Snake and Clearwater Rivers, respectively. Higher fine material content was found in the confluence zone near to the upstream corner (Braun et al. 2012).

2. METHODOLOGY

2.1 Water velocity and position measurements

A boat-mounted acoustic Doppler current profiler (ADCP) is a versatile tool for riverine studies that can provide measurements of velocity and channel topography. The ADCP measures 3D velocity components along a vertical profile by emitting acoustic pulses, called pings, along four beams. These pings move through the water column and reflect off of scatterers (suspended sediment and organic matter moving with the flow). The frequency shift between the sent and reflected pulses is used to calculate the flow velocity. Velocities from three beams are combined to provide 3D components while the fourth beam gives an estimate of measurement error. As shown in Figure 3, the water column is divided into equally-spaced depth cells, called bins, and the mean velocity from all pings reflected within each cell is placed at the bin center. The raw velocity measured by the ADCP includes contributions from the flowing water and motion of the boat. A measure of the boat velocity is required to isolate the flow velocity. The boat velocity may be determined using either a global positioning system (GPS) or bottom tracking. Bottom tracking measures the movement of the ADCP relative to the channel bed and is accomplished by sending a strong pulse that reflects off of the bed. In addition to providing the velocity of the ADCP, bottom tracking also measures the flow depth at each beam.

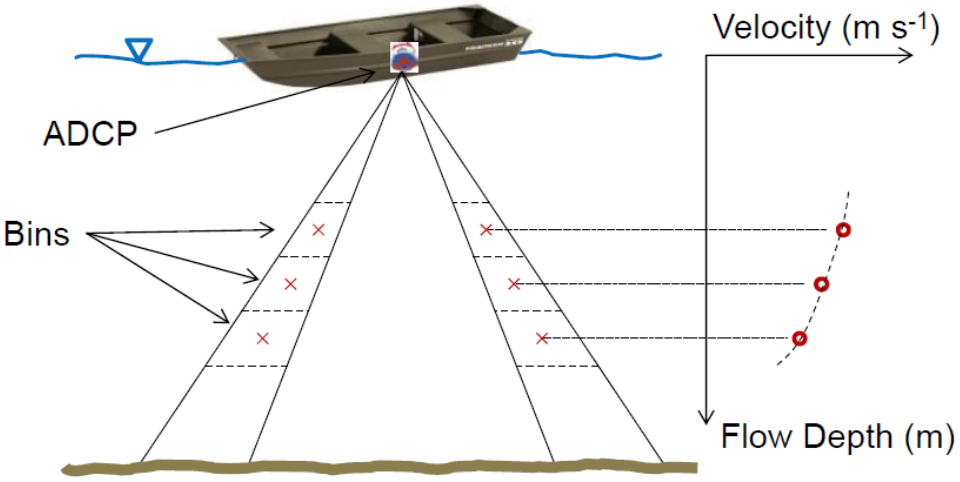

Figure 3: Illustration of a velocity profile measured by a boat-mounted ADCP. In addition to the two beams shown, the ADCP also emits beams into and out of the page.

The spatial and temporal resolution of the velocity measurements is dependent on the type of deployment. During moving-vessel (MV) measurements, the ADCP records continuously while the boat traverses the channel. This is the most common boat-mounted survey procedure and provides accurate measurements of discharge (Oberg & Mueller 2007). Fixed vessel (FV) measurements are performed while the boat is held at a constant position within the channel. The improved temporal resolution can be used to determine mean (e.g., time-averaged) velocity profiles (Petrie et al. 2013) and bed load velocity (Rennie et al. 2002).

Figure 4: equipment used in the field work.

The velocity field in the study area was measured using a Teledyne RDI 1200 kHz RiverPro ADCP installed in a RiverRay float and attached to the boat as shown in Figure 4. Positioning was provided by means of a R6-4 Trimble GPS installed directly above the ADCP and by using bottom tracking. The GPS accuracy was increased by acquiring corrections from Washington State Reference Network (WSRN). The GPS accuracy was tested by using two USGS bench marks, one in Pullman, WA (RZ1887) and the other is in Clarkston, WA near to the Post-confluence stream (RZ1076). The comparison between the GPS data and the USGS database showed that the margin of error is within few centimeters. A TruPulse200x Rangefinder (Figure 4) was used to measure the distances between the starting and ending ADCP positions to the river banks for MV measurement. These distances are essential to estimate discharge passing in the shallow regions near banks, which cannot be measured by the ADCP.

Figure 5 shows the outrigger configuration used to mount the ADCP to the boat. A square tube was placed across the boat width with its extra length extended on one side. The tube was fixed to the boat by elastic straps. The purpose of these square tube was to allow the RiverRay to be attached to the boat side at a distance far enough to prevent the GPS blockage. The RiverRay was connected to both the front and the rear of the boat to limit its movement.

Figure 5: The RiverRay mounted to the boat using an outrigger configuration.

Water velocity profiles were measured along 14 cross sections in the confluence region (Figure 6). These cross sections were selected to cover the entire confluent region including two cross sections up-stream of the confluence in each channel. The density of cross sections was increased in the confluence central zone to better capture the anticipated flow features. A minimum of four moving vessel measurements (transects) were taken at each of the 14 cross sections to enable a proper discharge estimate. A single transect was taken by starting at a location near to one bank and moving along the cross section to the other bank while the ADCP is recording the velocity profile. Also, FV measurements with durations ranging from 15 to 20 minutes were taken at different locations throughout the confluence to investigate the temporal velocity fluctuations.

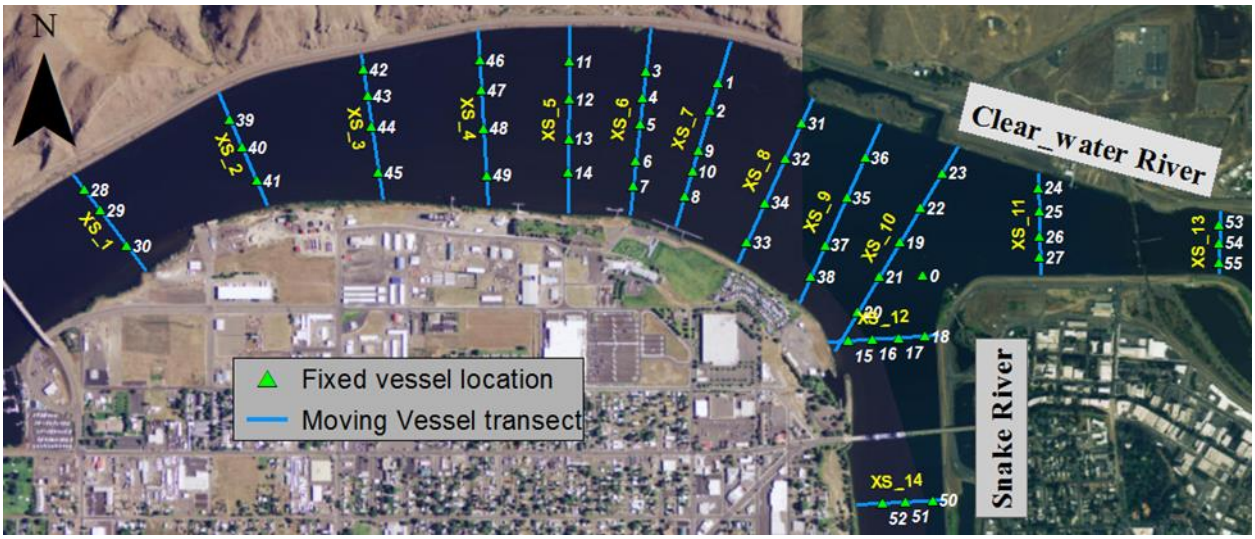

Figure 6: Moving vessel transects and fixed vessel locations

2.2 Sediment samplers

Measurement of bedload in rivers remains challenging due to the significant spatial and temporal variability of the phenomenon (Diplas et al. 2008). For example, laboratory experiments under steady flow required 40 to 50 minutes of sampling to obtain stable mean transport rates (Kuhnle & Southard 1988). Traditionally, bedload is measured by installing a trap-like device on the riverbed to collect the transported material. These intrusive samplers have the disadvantage of disturbing the near-bed flow field and bedload movement. More recently the ADCP, using the bottom tracking feature described previously, has been explored for nonintrusive measurements of bedload transport (Gaeuman & Jacobson 2006; Rennie et al. 2002).

A cable suspended Helley-Smith Sampler (Figure 7) was used to collect bed-load samples in the study area. A Helley-Smith Sampler consists of a metal frame and nozzle holding a mesh bag to collect samples. Helley-Smith samplers are usually deployed in non-wadeable rivers from a boat using a cable and winch. The basic operational procedure is to (1) lower the sampler onto the riverbed, (2) collect a bedload sample for some duration (typically 30 to 120 seconds), (3) raise the sampler off the bed and return it to the boat, and (4) empty the mesh bag. The contents of the mesh bag constitute the bedload sample and the transport rate can be computed from the sample weight and sampling duration while the sample grain size distribution can be determined by sieve

analysis. Due to the spatial and temporal variability of bedload, a large number of samples are typically required to quantify bedload transport rates at a site.

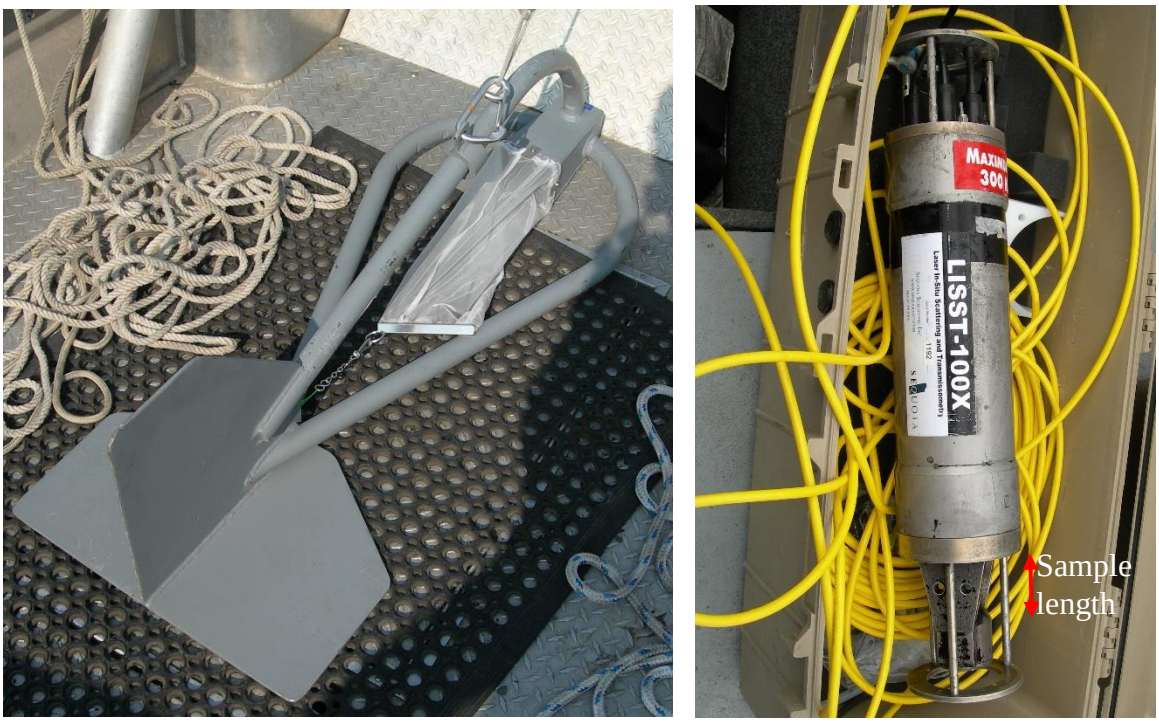

Figure 7: The Helley-Smith bedload sampler (left) and LISST-100X suspended load profiler (right)

Suspended load particle size and volume distributions were measured by a LISST-100X instrument produced by SEQUOIA (Figure 7). The LISST-100X works by sending a laser beam and receiving the reflections off of the suspended sediment particles over a ring of sensors known as a ring detector. The size of the particles is identified by the intensity of the reflected rays and the angle of reflection. The instrument was lowered slowly from the water surface to the river bottom to measure the suspended load distribution over the water column. The device continued measuring while it was lifted back to the boat to obtain another vertical profile (for comparison purposes). A suspended load measurement was taken at each ADCP FV measurement location.

2.3 Bathymetry survey

A 3DSS-DX-450 multi-beam sonar manufactured by Ping DSP (Figure 8) with a frequency of 450 kHz and beam width of 0.4^{o} was used to survey the bathymetry and identify the existent bed morphological elements throughout the confluence. This device is capable of creating high resolution bathymetry maps that resolve bed forms on the river bed even in shallow waters with depths less than 1.0 m. The 3DSS was mounted on a vertical rod to the side of the boat, so that the device is submerged at a known depth below water surface. The river bathymetry survey was performed in the form of overlapped lines, in which the boat was driven in straight paths maintaining an overlap between paths. The width of the line depends mainly on the water depth. The deeper the water column, the wider the area covered on one line.

Figure 8: The 3DSS-DX-450 multi-beam sonar

3 PRINCIPLE FINDINGS AND SIGNIFICANCE

3.1 Flow conditions during the field observations

The total discharge passing through the confluence during the study period ranged between 765 and 903 m^3/s as shown in Figure 9 **Error! Reference source not found.**. Discharge is measured at USGS stations 13342500 and 13334300. These two gaging stations are located at distances of 19 km and 46 km upstream from the confluence center in the Snake and the Clearwater Rivers, respectively. The corresponding discharge ratio in the confluence, $Q_r = Q_{Clearwater} / Q_{Snake}$, fluctuated between 0.56 and 1.0 during the same period. Low flow conditions were present during the study period, the aforementioned flow rates are low compared to the historic average daily flow during the same period, which was > 1260 m^3/s based on data from 2000 to 2014 (http://waterdata.usgs.gov) . This low flow is likely due to the significantly low snow pack and the relatively high temperatures in this year.

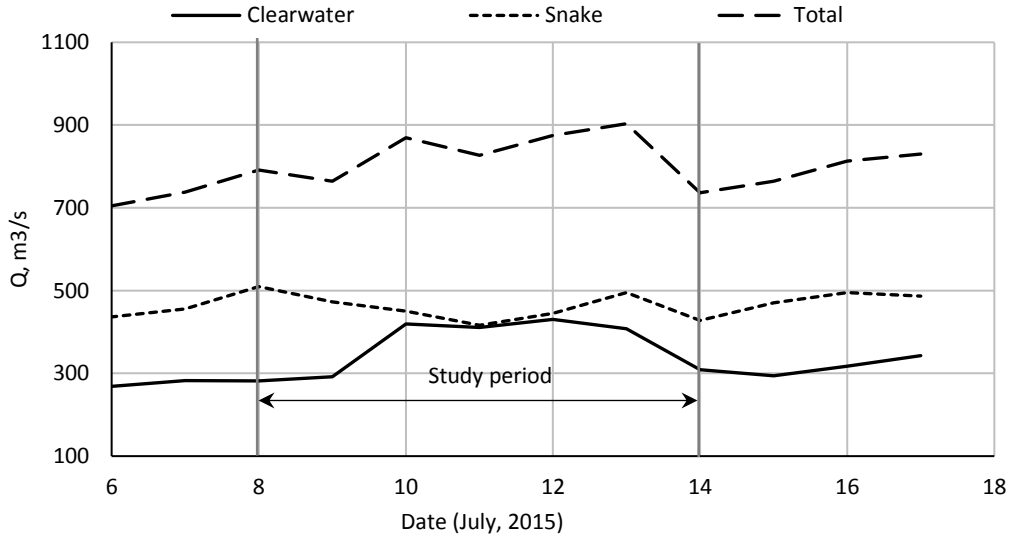

Figure 9: Discharge in the confluence during field measurements.

3.2 Confluence Bathymetry

The results of the bathymetry survey (**Error! Reference source not found.**) show that the maximum depths upstream of the confluence in the Snake and Clearwater Rivers were about 12 m and 7.5 m, respectively. Regions with higher depths (> 16 m) were observed in the vicinity of the upstream bridges, which can be attributed to scour around the bridge piers. The two river beds merge smoothly after entering the confluence creating little to no bed discordance. This observation is consistent with the results obtained in large braid-bar confluences (Szupiany et al. 2009).

Large areas with relatively shallow depths (< 6 m) were observed around the confluence upstream corner, and for a long distance next to the post-confluence left bank starting from the downstream corner and continuing beyond XS_3. This finding could indicate the formation of sediment bars. The confluence thalweg and the surrounding deep region (> 11 m) began as a wide region in the Snake River and then reduced in size and depth at the center of the confluence. Further downstream in the vicinity of XS_5, the thalweg increases in size and depth as it extends through the confluence moving towards the outer bank (right bank facing downstream). Large bed forms develop at the edge of the deep region starting from within the Snake River to the downstream end of the study area. Smaller separated patches with depths > 11 m were also observed in the confluence central zone near the outer bank.

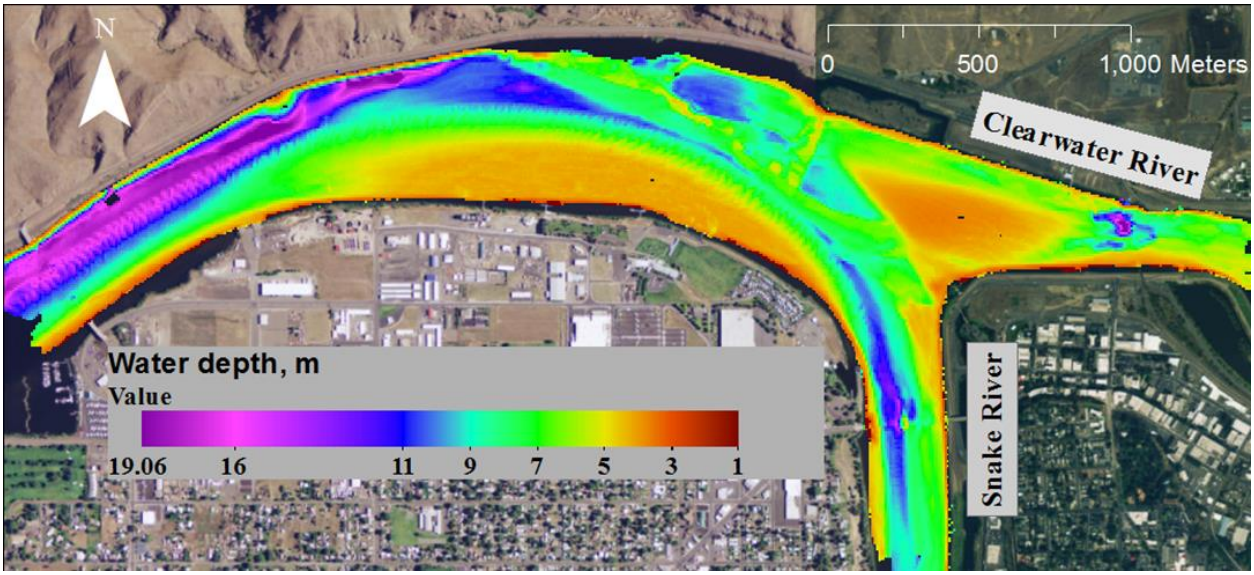

Figure 10: Confluence morphology measured on July, 9th 2015 (vertical datum is the water surface).

3.3 Sediment measurements

The Helley-Smith sampler was used to obtain bedload samples from the confluence region. Two sampling durations of 5 and 60 minutes were tested in locations near to the confluence center (locations expected to have the most bed load transport). No significant bedload was detected in either sample. Additionally, the ADCP bottom track data indicated that the bed was not moving. These observations demonstrate that little to no bedload was present in the test region. This finding is attributed to the significantly low snow pack and resulting low flow conditions through the confluence in the spring of 2015. The processing of the suspended load measurements is in

progress to establish the role of hydrodynamics on mixing of suspended sediment within the confluence.

3.4 Depth-averaged velocity

The moving vessel transects were analyzed using the Velocity Mapping Toolbox (VMT) software (Parsons et al. 2013). The average of all transects taken at each cross section was used to compute the depth-averaged velocity distribution presented in Figure 11 for the 14 cross sections. The cross section average flow velocity in the Clearwater River was ~0.4 m/s at XS_13 and reduced to ~0.25 m/s at XS_11 before entering the confluence due to the increase in the river cross section. The cross section averaged velocity in the Snake River was about 0.25 m/s at XS_14. At the entrance to the confluence, the velocity increases in the region near to the right bank to ~0.35 m/s (see XS_12 in Figure 11). A region of higher velocity starts to develop initially in the confluence central zone near to the shear layer. Further downstream, the maximum velocity region shifts towards the right bank and increases in magnitude, reaching a peak at XS_8 with average velocities > 0.45 m/s. The velocity decreases downstream of XS_8 to a more homogenous average velocity distribution as the mixing interface between the two flows diminishes.

Low velocities with magnitudes < 0.1 m/s were observed along the left bank starting from the confluence downstream corner. In this region, depth-averaged velocities moving upstream were also seen near the left bank in some transects at XS_4 and XS_5. These features may be due to flow deflection around the relatively sharp change in the bank alignment occurring near XS_6. This result indicates the formation of a separation zone in the vicinity of the confluence downstream corner and after the change in bank alignment. The aforementioned flow characteristics and patterns agree with the general hydrodynamics model proposed by Best (1987).

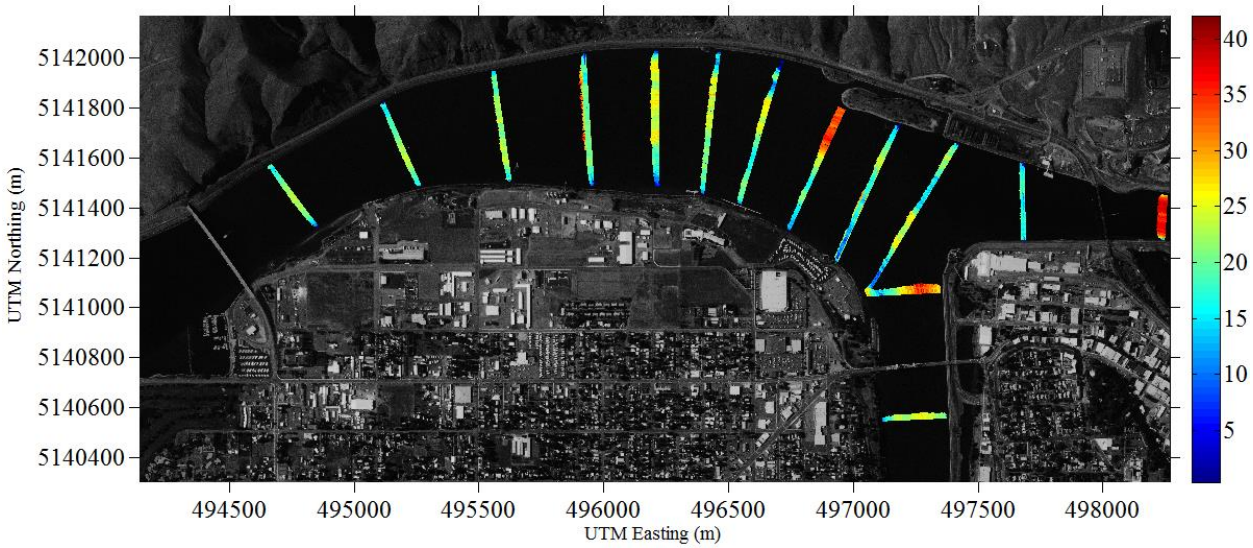

Figure 11: Depth-averaged velocity (cm/s) measured at cross sections in the vicinity of the confluence.

3.5 Secondary circulation

Analysis of the cross stream velocity components was performed using the zero net cross-stream discharge technique. This technique defines the direction of primary flow to minimize secondary

discharge over the whole cross section (Paice 1990). The results demonstrate the development of a clockwise circulation cell (looking downstream) in the Snake River side starting from XS_10 with cross-stream velocity magnitudes comparable to the streamwise velocities that reach magnitudes > 0.35 m/s in some regions (Figure 12a). No significant circulation cells were observed on the Clearwater side at that cross section. This finding may be due to the relatively low velocity field in the Clearwater River entering the confluence compared to the Snake River. As the flow moves further downstream, the circulation cell expands towards the right bank until it includes the majority of the cross section at XS_8 (Figure 12b). The cross stream velocity magnitudes decrease to < 0.22 m/s at XS_8. Further downstream, the circulation cell dissipates as the flow recovers (Figure 12c). The secondary circulation in the vicinity of XS_8 is similar to that observed in meander bends.

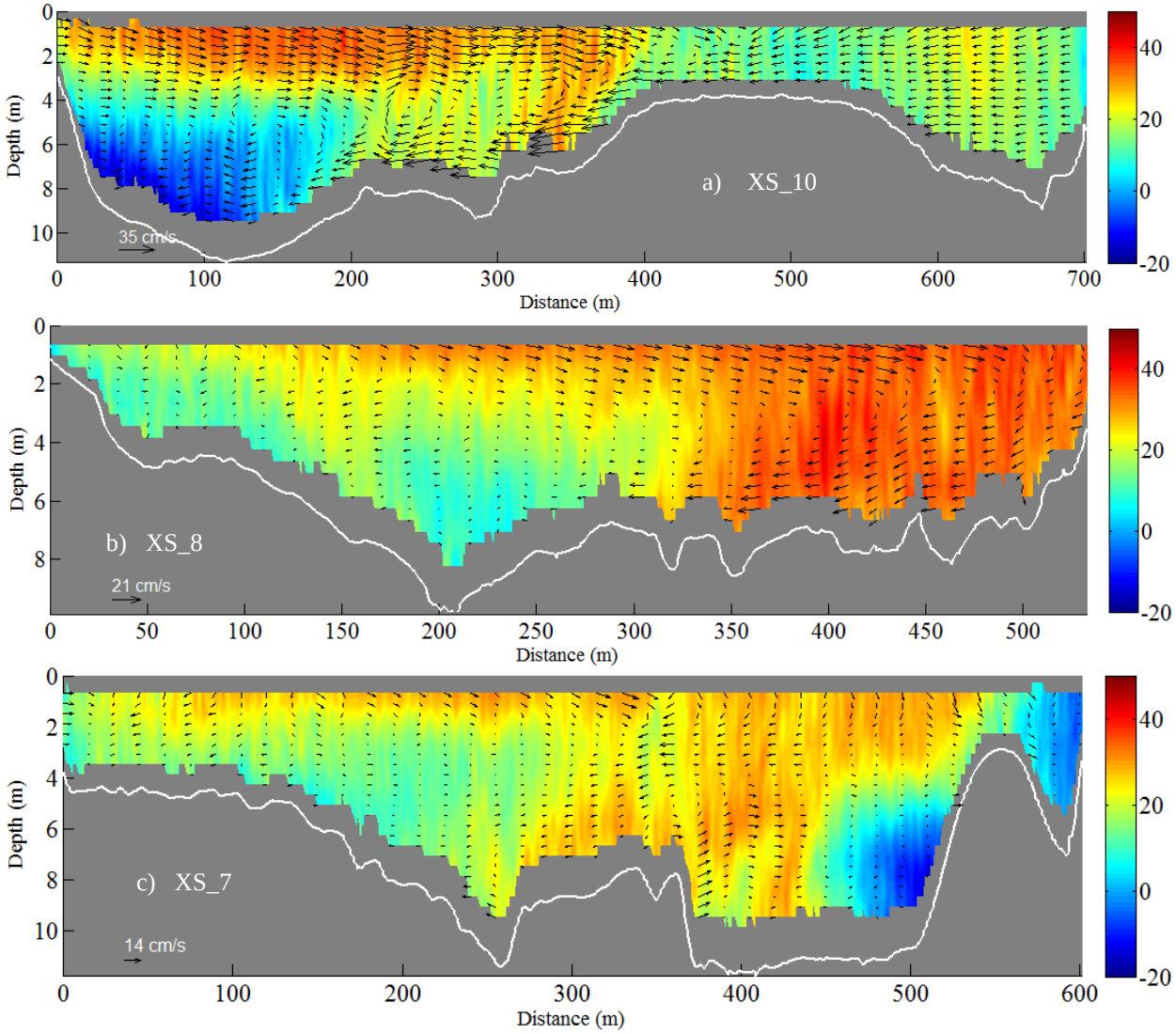

Figure 12: Cross-stream velocity vectors (cm/s) and contours of stream wise velocity (cm/s) at different cross sections in the post-confluence region (facing downstream).

The low flow occurring during measurements is not expected to be significantly responsible for the confluence morphology. Also, the confluence morphology is systemically influenced by dredging operations. However, the measured flow patterns generally agree with the bed bathymetry. Low velocity regions at both the confluence upstream and downstream corners existed in the shallowest flow depths. The maximum velocities were observed in the regions characterized with high flow depths. The secondary circulation pattern is also consistent with the meander planform morphology in the Snake River.

4 LIST OF STUDENTS SUPPORTED

- Mahmoud Shehata, a Washington State University PhD student. Mahmoud participated in collecting and taking the field measurements. He processed the measurement data and prepared the publications under guidance of the PI.
- Gregory Moore, a Washington State University undergraduate student. Gregory participated in setting up and testing the equipment used in the field work.

5 REFERENCES

Benda, L., Poff, N.L., Miller, D., Dunne, T., Reeves, G., Pess, G., & Pollock, M. (2004). The network dynamics hypothesis: how channel networks structure riverine habitats. BioScience *54*, 413–427.

Best, J.L. (1986). The morphology of river channel confluences. Prog. Phys. Geogr. *10*, 157–174.

Best, J.L. (1987). Flow Dynamics at River Channel Confluences: Implications for Sediment Transport and Bed Morphology. Recent Dev. Fluv. Sedimentol. *39*, 27–35.

Best, J.L. (1988). Sediment transport and bed morphology at river channel confluences. Sedimentology *35*, 481–498.

Best, J.L., & Rhoads, B.L. (2008). Sediment transport, bed morphology and the sedimentology of river channel confluences. River Conflu. Tribut. Fluv. Netw. 45–72.

Biron, P., Roy, A., Best, J.L., & Boyer, C.J. (1993). Bed morphology and sedimentology at the confluence of unequal depth channels. Geomorphology *8*, 115–129.

Biron, P.M., Richer, A., Kirkbride, A.D., Roy, A.G., & Han, S. (2002). Spatial patterns of water surface topography at a river confluence. Earth Surf. Process. Landf. *27*, 913–928.

Boll, J., Brooks, E., McAtty, J., Barber, M., Ullman, J., McCool, D., Lu, X., Lawler, A., & Ryan, J. (2010). Evaluation of sediment yield reduction potential in agricultural and mixed-use watersheds of the Lower Snake River basin (Pullman, WA: submitted to US Army Corps of Engineers by State of Washington Water Research Center).

Boyer, C., Roy, A.G., & Best, J.L. (2006). Dynamics of a river channel confluence with discordant beds: Flow turbulence, bed load sediment transport, and bed morphology. J. Geophys. Res. Earth Surf. *111*, F04007.

Bradbrook, K.F., Lane, S.N., & Richards, K.S. (2000). Numerical simulation of three-dimensional, time-averaged flow structure at river channel confluences. Water Resour. Res. *36*, 2731–2746.

Braun, C.L., Wilson, J.T., Van Metre, P.C., Weakland, R.J., Fosness, R.L., & Williams, M.L. (2012). Grain-size distribution and selected major and trace element concentrations in bed-sediment cores from the Lower Granite Reservoir and Snake and Clearwater Rivers, eastern Washington and northern Idaho, 2010 (US Department of the Interior, US Geological Survey).

Clark, G.M., Fosness, R.L., & Wood, M.S. (2013). Sediment Transport in the Lower Snake and Clearwater River Basins, Idaho and Washington, 2008-11 (US Geological Survey).

Constantinescu, G., Miyawaki, S., Rhoads, B., Sukhodolov, A., & Kirkil, G. (2011). Structure of turbulent flow at a river confluence with momentum and velocity ratios close to 1: Insight provided by an eddy-resolving numerical simulation. Water Resour. Res. *47*, W05507.

Constantinescu, G., Miyawaki, S., Rhoads, B., & Sukhodolov, A. (2012). Numerical analysis of the effect of momentum ratio on the dynamics and sediment-entrainment capacity of coherent flow structures at a stream confluence. J. Geophys. Res. Earth Surf. *117*, F04028.

Diplas, P., Kuhnle, R., Gray, J., Glysson, D., & Edwards, T. (2008). Sediment Transport Measurements. In Sedimentation Engineering, (American Society of Civil Engineers), pp. 307–353.

Gaeuman, D., & Jacobson, R.B. (2006). Acoustic bed velocity and bed load dynamics in a large sand bed river. J. Geophys. Res. Earth Surf. *111*, F02005.

Kuhnle, R.A., & Southard, J.B. (1988). Bed load transport fluctuations in a gravel bed laboratory channel. Water Resour. Res. *24*, 247–260.

Lane, S.N., Parsons, D.R., Best, J.L., Orfeo, O., Kostaschuk, R.A., & Hardy, R.J. (2008). Causes of rapid mixing at a junction of two large rivers: Río Paraná and Río Paraguay, Argentina. J. Geophys. Res. Earth Surf. *113*, F02024.

Leite Ribeiro, M., Blanckaert, K., Roy, A.G., & Schleiss, A.J. (2012). Flow and sediment dynamics in channel confluences. J. Geophys. Res. Earth Surf. *117*, F01035.

Mosley, M.P. (1976). An Experimental Study of Channel Confluences. J. Geol. *84*, 535–562.

Oberg, K., & Mueller, D.S. (2007). Validation of streamflow measurements made with acoustic Doppler current profilers. J. Hydraul. Eng. *133*, 1421–1432.

Paice, C. (1990). Hydraulic control of river bank erosion: an environmental approach. University of East Anglia.

Parsons, D.R., Best, J.L., Lane, S.N., Kostaschuk, R.A., Hardy, R.J., Orfeo, O., Amsler, M.L., & Szupiany, R.N. (2008). Large river channel confluences. In River Confluences, Tributaries and the Fluvial Network, pp. 17–32.

Parsons, D.R., Jackson, P.R., Czuba, J.A., Engel, F.L., Rhoads, B.L., Oberg, K.A., Best, J.L., Mueller, D.S., Johnson, K.K., & Riley, J.D. (2013). Velocity Mapping Toolbox (VMT): a processing and visualization suite for moving-vessel ADCP measurements. Earth Surf. Process. Landf. *38*, 1244–1260.

Petrie, J., Diplas, P., Gutierrez, M., & Nam, S. (2013). Data evaluation for acoustic Doppler current profiler measurements obtained at fixed locations in a natural river. Water Resour. Res. *49*, 1003–1016.

Rennie, C.D., Millar, R.G., & Church, M.A. (2002). Measurement of Bed Load Velocity using an Acoustic Doppler Current Profiler. J. Hydraul. Eng. *128*, 473–483.

Rhoads, B.L. (1996). Mean structure of transport-effective flows at an asymmetrical confluence when the main stream is dominant. Coherent Flow Struct. Open Channels 491–517.

Rhoads, B.L., & Kenworthy, S.T. (1998). Time-averaged flow structure in the central region of a stream confluence. Earth Surf. Process. Landf. *23*, 171–191.

Rhoads, B.L., & Sukhodolov, A.N. (2001). Field investigation of three-dimensional flow structure at stream confluences: 1. Thermal mixing and time-averaged velocities. Water Resour. Res. *37*, 2393–2410.

Rice, S., Roy, A., & Rhoads, B. (2008). River confluences, tributaries and the Fluvial Network (John Wiley & Sons).

Sukhodolov, A.N., & Rhoads, B.L. (2001). Field investigation of three-dimensional flow structure at stream confluences: 2. Turbulence. Water Resour. Res. *37*, 2411–2424.

Szupiany, R.N., Amsler, M.L., Parsons, D.R., & Best, J.L. (2009). Morphology, flow structure, and suspended bed sediment transport at two large braid-bar confluences. Water Resour. Res. *45*, W05415.

USACE (2014). Executive Summary Lower Snake River Draft Programmatic Sediment Management Plan – Final EIS.